Metal-to-Ligand Charge Transfer Excited-State ν(CO) Shifts in Rigid Media

Dana M. Dattelbaum and Thomas J. Meyer*

Department of Chemistry, CB 3290, University of North Carolina at Chapel Hill, Chapel Hill, North Carolina 27599-3290, and Los Alamos National Laboratory, MS A127, Los Alamos, New Mexico 87545

Received: November 5, 2001; In Final Form: February 6, 2002

The results of ν(CO) infrared measurements on the ground and metal-to-ligand charge transfer (MLCT) excited states of *fac*-[Re^{I}(4,4′-X$_2$bpy)(CO)$_3$(4-Etpy)]$^+$ (X = H, CH$_3$, and CO$_2$Et; 4-Etpy is 4-ethylpyridine) in both CH$_3$CN and poly(methyl methacrylate) (PMMA) films at 298 K are reported. In PMMA, the shifts in ν(CO) between the excited and ground states (+18 to +68 cm^{-1}) are noticeably less than in solution (+33 to +88 cm^{-1}). Our work was stimulated by the observation by Turner and co-workers (*Chem. Commun.* **1996**, 1587−1588) that ν(CO) excited-to-ground-state shifts for *fac*-[Re(bpy)(CO)$_3$Cl] are much less in a rigid butyronitrile/propionitrile glass at 77 K than in CH$_3$CN at 298 K. For the Re complexes, a single correlation exists between excited-state ν(CO) shifts and the MLCT ground-to-excited-state energy gap (E_0) regardless of whether the energy gap is changed by varying the substituent X or the medium. The substituent and rigid medium effects appear to have a common orbital origin arising from π^*(4,4′-X$_2$bpy$^{\bullet-}$)−π^*(CO) mixing. This provides the orbital basis for mixing higher lying dπ(Re)−π^*(CO) MLCT states with the emitting dπ(Re)−π^*(4,4′-X$_2$-bpy$^{\bullet-}$) MLCT excited state(s).

Introduction

A characteristic feature in the infrared spectra of CO-containing metal-to-ligand charge transfer (MLCT) excited states is an increase in excited-state ν(CO) band energies compared to the ground state.[1−6] For *cis*-[Os(bpy)$_2$(CO)(Cl)]$^{+}$* (eq 1), $\bar{\nu}$(CO) = 2022 cm^{-1} in the excited state ($\bar{\nu}_{es}$) and 1948 cm^{-1} in the ground state ($\bar{\nu}_{gs}$) with a difference, $\Delta\bar{\nu}$(CO) ($=\bar{\nu}_{es} - \bar{\nu}_{gs}$), of 75 cm^{-1} in CH$_3$CN at 298 K.[7] In the pseudo-C_{3v} symmetry of *fac*-[Re(bpy)(CO)$_3$(4-Etpy)]$^+$ there are two ground-state ν(CO) bands arising from an A$_1$ mode and a degenerate pair of E modes. All three shift to higher energy in the C_s symmetry of the MLCT excited state with ground-to-excited-state shifts of $\Delta\bar{\nu}$ = +44, +83, and +39 cm^{-1} (eq 2).[7] These excited "states" are actually a set of three low-lying, Boltzmann-populated states largely triplet in character having a common dπ^5−π^{*1} orbital origin.[8−12]

$$cis\text{-}[Os^{II}(bpy)_2(CO)(Cl)]^+ \xrightarrow{h\nu} cis\text{-}[Os^{III}(bpy^{\bullet-})(bpy)(CO)(Cl)]^{+}* \quad (1)$$

$$fac\text{-}[Re^{I}(bpy)(CO)_3(4\text{-}Etpy)]^+ \xrightarrow{h\nu} fac\text{-}[Re^{III}(bpy^{\bullet-})(CO)_3(4\text{-}Etpy)]^{+}* \quad (2)$$

Correlations have been found between excited-state ν(CO) band energies and the MLCT excited-to-ground-state energy gap (E_0) for a series of Os and Re polypyridyl complexes.[7] Variations in $\bar{\nu}_{es}$ induced by changes in the ancillary or acceptor ligands have been attributed to changes in dπ(M)−π^*(CO) back-bonding, polarization of the σ(M−CO) bond, dπ(M)−π(bpy) mixing, and π^*(bpy)−π^*(CO) mixing.

For the MLCT excited state(s) of *fac*-[Re(bpy)(CO)$_3$Cl], Turner and co-workers[13] reported a dramatic decrease in the ground-to-excited-state shift in ν(CO) at the fluid-to-glass transition in a 5:4 butyronitrile/propionitrile mixture. They attributed the decrease to enhanced mixing between the lowest MLCT excited state and low-lying bpy-based $\pi\pi^*$ excited states in the rigid glass.

The ν(CO) effect, which has been termed infrared "rigidochromism", is reminiscent of a phenomenon first described by Wrighton and Morse and subsequently confirmed by many others.[14−24] They observed an increase in MLCT emission energy in rigid compared to fluid media. It has been shown that ligand-localized $\pi\pi^*$ excited-state energies in related complexes are relatively unaffected by the transition from fluid to glass.[23,25]

We report here the results of a study related to that of Turner and co-workers[13] but at room temperature in poly(methyl methacrylate) (PMMA) films for the series *fac*-[Re^{I}(4,4′-X$_2$-bpy)(CO)$_3$(4-Etpy)]$^+$ (X = CH$_3$, H, CO$_2$Et). The acquisition of excited-state data in PMMA is itself notable since this appears to be the first example of transient infrared (TRIR) spectra of transition metal complexes recorded in a polymeric film.

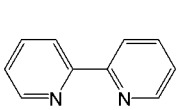

bpy

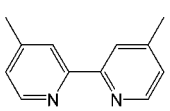

4,4'-(CH$_3$)$_2$bpy

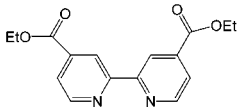

4,4'-(CO$_2$Et)$_2$bpy

Experimental Section

Materials. Low molecular weight (10 000−15 000 amu) poly(methyl methacrylate) (PMMA) was purchased from Aldrich and used as received. Chloroform and acetonitrile were purchased from Burdick and Jackson, and acetone was purchased from Mallinckrodt. All were used as received. The salts *fac*-[Re^{I}(4,4′-X$_2$bpy)(CO)$_3$(4-Etpy)](PF$_6$) were prepared in several steps from Re(CO)$_5$Cl according to literature procedures.[26−28]

* Corresponding author: tjmeyer@lanl.gov.

10.1021/jp014057z CCC: $22.00
Published on Web 04/17/2002

IR and TRIR spectra were recorded in a gastight liquid cell consisting of two BaF_2 plates separated by a 0.75 mm Teflon spacer purchased from Harrick.

Preparation of Polymer Films. PMMA (0.5 g) was dissolved in 5 mL of chloroform. This solution was added to a 1 mL solution of the complex in acetonitrile, with the concentration adjusted so that the absorbance of the CO bands was ~0.7; the mixture was stirred and poured into a Teflon mold. The solvent was allowed to evaporate slowly over a period of 2−3 days. The polymer film was placed under vacuum in a desiccator for another 2 days prior to measurements. The films produced by this method were 4 cm in length and 1 cm wide with a relatively uniform thickness of ~0.8 mm.

IR and TRIR Spectra. Samples for TRIR measurements were prepared in fresh acetonitrile, with the concentration adjusted so that the absorbance of the CO bands was ~0.7−1.0 (air background). TRIR spectra in CH_3CN were recorded at an absorbance of ~0.8. After incorporation in PMMA, sample absorbances were at ~1.0−1.2. At absorbances greater than 1.2, spikelike artifacts appeared in the TRIR spectra.

PMMA films were mounted on the back half of a typical liquid cell mount with adhesive tape with the IR beam passing through the center of the film. The films were mounted with a slight tilt away from perpendicular to the incident IR beam in order to minimize etalon effects.

A diagram of the apparatus for obtaining time-resolved infrared spectra in the mid-IR region is available as Figure A in the Supporting Information. Ground-state IR and TRIR spectra were recorded on a Bruker IFS 66V/s step-scan Fourier transform infrared (FTIR) spectrometer. Ground-state spectra were recorded in the rapid-scan mode and excited-state spectra in the step-scan mode. The infrared beam from the interferometer was directed through a BaF_2 window in a flange at the front of the bench, directed by a gold-coated mirror, and focused onto the sample by BaF_2 lenses. The diverging beam post-sample was recollimated and directed onto the detector element of a Kolmar liquid N_2-cooled MCT photovoltaic detector with a fast (50 MHz) preamplifier. For the CO region, a Ge low-pass filter with a 2250 cm^{-1} cutoff was mounted in front of the detector. A 354.7 nm pump beam from a Surelite Continuum Nd:YAG laser operating at 10 Hz was focused and directed onto the sample and overlapped with the infrared beam by using a pinhole aperture. The external optical train was enclosed in a plexiglass box that was continuously purged with dry N_2. Both the detector and sample were mounted on *x*, *y*, *z* translational stages for maximum alignment capability. Experimental timing of the laser pulse and interferometer mirror step was provided by a Sanford Research Systems Model DG535 pulse generator.

An AC rapid-scan single-channel spectrum was recorded prior to the step-scan experiment and used as the reference ground-state spectrum, $I(\upsilon)$. Time-resolved spectra were recorded in step-scan mode by using the PAD 82a transient ADC board. The AC signal from the photovoltaic MCT detector was fed into channel A of the PAD 82a transient digitizer board. The DC signal was fed into channel B and software-controlled to generate a static interferogram with its associated computed phase file. This DC-signal phase file was subsequently used to phase-correct the AC-coupled transient interferogram generated by channel A. Channel C received a trigger signal from the pulse generator to start data collection at each mirror step. Signal intensities were collected in 20 or 50 ns time increments to approximately 600 ns. Laser excitation reached the sample 324 ns after the mirror settled and the trigger delay feature was often used to postpone data collection until just prior to laser excitation. In-step coadditions (64−180) were used to increase the signal/noise ratio. Following the completion of an experiment, interferograms were Fourier-transformed and sorted in time to produce a 3D data set of single-channel spectra. The 3D file was further manipulated by a macro that converted the single-channel spectra into absorbance spectra by using the relationship $\Delta A = -\log [1 + I(\upsilon, t)/I(\upsilon)]$. In this expression, $I(\upsilon, t)$ and $I(\upsilon)$ are the infrared intensities at time t from the 3D file and at time = 0, respectively.[29] Time slices following the laser pulse were signal-averaged over the lifetime of the excited state to produce the final spectra.

Emission. Steady-state emission spectra were recorded on a Spex Fluorolog-212 spectrofluorometer equipped with a 450 W Xe lamp and a cooled 10-stage Hammamatsu R928 or R664 photomultiplier. Spectra were collected at right-angle geometry and were corrected for instrument response by using correction factors obtained with a NIST-calibrated standard lamp (Optronics Laboratories, Inc., model 220M) controlled by a precision current source at 6.50 W (Optronics Laboratories, Inc., model 65). The manufacturer's recommendations regarding lamp geometry were followed. Solution spectra were acquired in CH_3CN at room temperature in a 1 cm path length quartz cell (OD < 0.05) purged with argon. PMMA films were held in the quartz cell with a small Teflon piece cut specifically for the cuvette, notched to hold the polymer film. Films were angled away from the PMT to minimize reflectance of excitation light into the PMT.

Excitation was at 370 nm, with light from a Xe lamp as the excitation source. Emission was monitored from 400 to 700 nm. The emission spectra were fitted by using an in-house emission spectral fitting program based on a single-mode Franck−Condon analysis of spectral profiles described previously.[30,31] E_0, the excited-to-ground-state energy gap, is the energy maximum for the $\upsilon' = 0 \rightarrow \upsilon = 0$ vibronic component, $\Delta\bar{\nu}_{1/2}$ is the bandwidth at half-height, and S is the electron-vibrational coupling constant or Huang−Rhys factor. In the fits, $\hbar\omega$ was held at 1450 cm^{-1}, which is an average reflecting contributions from a series of medium-frequency ring-stretching modes and the 2040 cm^{-1} ν(CO) mode as assessed from resonance Raman spectra.[26]

Results

Time-resolved infrared (TRIR) spectra in the ν(CO) region from 1800 to 2300 cm^{-1} were acquired in acetonitrile and PMMA. Ground and TRIR spectra for *fac*-$[Re^{I}(bpy)(CO)_3(4\text{-Etpy})]^+$ (4-Etpy is 4-ethylpyridine) in CH_3CN are shown in Figure 1 and for *fac*-$[Re^{I}(4,4'\text{-}X_2bpy)(CO)_3(4\text{-Etpy})]^+$ (X = H and CO_2Et) in PMMA in Figure 2 and Figure B in the Supporting Information. The results are summarized in Table 1.

Emission spectra were also acquired in acetonitrile and PMMA. As described in the Experimental Section, the spectra were analyzed by application of a standard Franck−Condon analysis and use of the average mode approximation. In the fits, the quantum spacing for the average mode was fixed at 1450 cm^{-1}.[26] The remaining parameters in the fits were (1) the electron-vibrational coupling constant or Huang−Rhys factor (S), which is related to the square of the change in equilibrium displacement between excited and ground states, ΔQ_{eq}; (2) the bandwidth at half-height ($\Delta\bar{\nu}_{1/2}$), which includes the solvent and low-frequency modes treated classically; and (3) the $\upsilon' = 0 \rightarrow \upsilon = 0$ energy gap, E_0.[32] Emission energies and spectral fitting parameters are summarized in Table 2. A representative emission spectrum, for *fac*-$[Re^{I}(bpy)(CO)_3(4\text{-Etpy})]^{+*}$ in PMMA, is shown in Figure C in the Supporting Information.

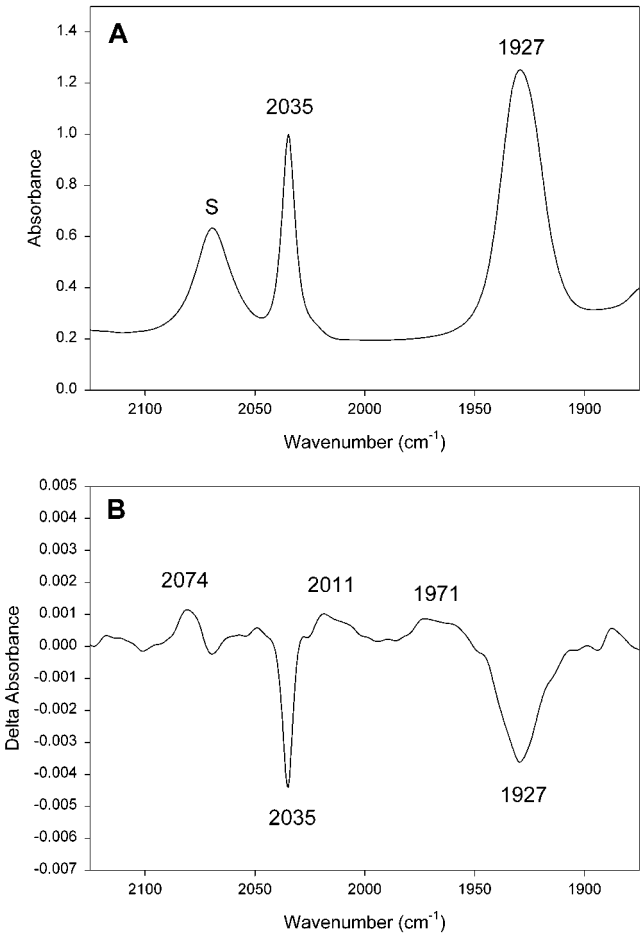

Figure 1. Ground (A) and time-resolved (B) infrared spectra of *fac*-[Re^{I}(bpy)(CO)$_3$(4-Etpy)]$^+$ in CH_3CN at 298 K in the CO region. S labels a solvent band.

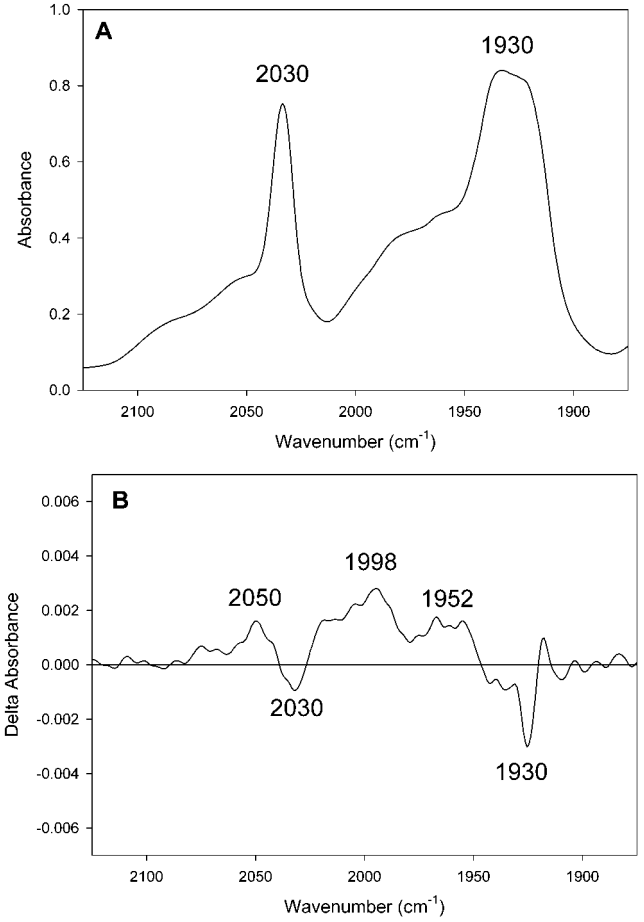

Figure 2. Ground (A) and time-resolved (B) infrared spectra of *fac*-[Re^{I}(bpy)(CO)$_3$(4-Etpy)](PF$_6$) in PMMA at 298 K in the ν(CO) region. The periodic noise in the TRIR spectrum is an etalon effect between the impinging IR beam and the PMMA film.

Discussion

In the study of Turner and co-workers,[13] it was noted that the fluid-to-glass transition in a 5:4 (v/v) butyronitrile/propionitrile mixture at 77 K had a profound effect on the magnitude of the excited-to-ground-state ν(CO) shifts in *fac*-[Re^{I}(bpy)(CO)$_3$Cl]. As noted in the Introduction, there is a general tendency for ν(CO) band energies to increase in MLCT excited states because partial oxidation at the metal decreases dπ(Re)$-\pi^*$(CO) back-bonding.[1,3−6] σ(M−CO) bond polarization may also play a role.[7]

Turner and co-workers[13] reported that the MLCT excited-state increase in ν(CO) in a frozen nitrile glass at 77 K was much less than in fluid solution. They attributed this effect to an increase in excited-state energy in the rigid medium, which caused enhanced MLCT excited-state mixing with low-lying $\pi\pi^*$(bpy) excited states. This is a reasonable suggestion because in related Re complexes ligand-localized and MLCT excited states are known to lie in close proximity with the state ordering depending on the ligands, the medium, and the temperature.[14,25−27,33−46] Our results demonstrate that a related rigid medium effect exists for *fac*-[Re^{I}(bpy)(CO)$_3$(4-Etpy)]$^+$, *fac*-[Re^{I}(4,4′-(CH$_3$)$_2$bpy)(CO)$_3$(4-Etpy)]$^+$, and *fac*-[Re^{I}(4,4′-(CO$_2$Et)$_2$bpy)(CO)$_3$(4-Etpy)]$^+$ in rigid PMMA films at room temperature (Table 1).

Effect of Rigid Media on the Energy Gap. The increases in emission energy (E_{em}) and energy gap (E_0) between fluid and rigid media are well documented for MLCT excited states.[14−24] They are caused by the frozen character of the orientational part of the solvent dielectric. Except for very short-lived excited states, emission in fluid solution occurs with the full dielectric polarization equilibrated with the electronic configuration of the excited state.

In treating this problem theoretically, Marcus divided the medium reorganization energy into frozen, λ_{oo}, and unfrozen, λ_{io}, parts (eq 3).[47−49] ΔG°_{es} is the free energy content of the excited state above the ground state in rigid (frozen), ΔG°_{es}(fr), or fluid solution, ΔG°_{gs}(fl).

$$\lambda_o = \lambda_{oo} + \lambda_{io} \tag{3}$$

$$\Delta G^\circ_{es}(\mathrm{fr}) = \Delta G^\circ_{gs}(\mathrm{fl}) + \lambda_{oo} \tag{4}$$

In a rigid medium, the orientational part of the dielectric, λ_{oo}, becomes part of the free energy change and no longer contributes to the reorganizational energy. This increases the free energy of the excited state above the ground state over that in the fluid by λ_{oo} (eq 4).[50]

This λ_{oo} increase in emission energy compared to fluid solution is the origin of the rigid medium effect for MLCT emission. In the dipole-in-a-sphere model, λ_{oo} depends on the squared difference between excited-state and ground-state vector dipole moments ($\vec{\mu}_f$, $\vec{\mu}_i$), the static dielectric constants in frozen ($D_{s,fr}$) and fluid ($D_{s,fl}$) media, and the radius of the sphere (a):

$$\lambda_{oo} = \frac{(\vec{\mu}_f - \vec{\mu}_i)^2}{a^3}\left[\frac{1 - D_{s,fr}}{2D_{s,fr} + 1} - \frac{1 - D_{s,fl}}{2D_{s,fl} + 1}\right] \tag{5}$$

For a $\pi\pi^*$ excited state, $\vec{\mu}_f \sim \vec{\mu}_i$ and the fluid-to-glass effect

TABLE 1: Ground-State IR ($\bar{\nu}_{gs}$) and TRIR ($\bar{\nu}_{es}$) ν(CO) Data for *fac*-[Re^{I}(4,4′-X$_2$bpy)(CO)$_3$(4-Etpy)]$^+$ in CH$_3$CN and PMMA at 298 K

		$\bar{\nu}_{gs}$, cm^{-1}		$\bar{\nu}_{es}$, cm^{-1}					
complex[a]	medium	E	A$_1$	A″	A′(2)	A′(1)	$\Delta\bar{\nu}$,[b] cm^{-1}	$\Delta\Delta\bar{\nu}$,[c] cm^{-1}	E$_0$,[d] cm^{-1}
[Re^{I}(4,4′-(CH$_3$)$_2$bpy)(CO)$_3$(4-Etpy)]$^+$	CH$_3$CN	1927	2034	1965	2008	2067	+37, +81, +33		18 600
	PMMA	1931	2031	1950	2000	2045	+18, +68, +14	−19, −13, −19	20 400
[Re^{I}(bpy)(CO)$_3$(4-Etpy)]$^+$	CH$_3$CN	1927	2035	1971	2011	2074	+44, +84, +39		17 800
	PMMA	1930	2030	1952	1998	2050	+22, +68, +20	−19, −13, −24	20 000
[Re^{I}(4,4′-(CO$_2$Et)$_2$bpy)(CO)$_3$(4-Etpy)]$^+$	CH$_3$CN	1933	2038	1978	2023	2092	+45, +88, +54		16 200
	PMMA	1932	2034	1960	2000	2064	+28, +68, +30	−17, −20, −24	18 400

[a] As PF_6^- salts. [b] $\Delta\bar{\nu} = \bar{\nu}_{es} - \bar{\nu}_{gs}$. [c] $\Delta\Delta\bar{\nu} = \Delta\bar{\nu}_{PMMA} - \Delta\bar{\nu}_{CH_3CN}$. [d] Energy gap from Table 2.

TABLE 2: Emission Energies (E_{em}) and Spectral Fitting Parameters at 298 K in CH$_3$CN and PMMA[a]

complex[b]	medium	E_0,[b] cm^{-1}	E_{em}, cm^{-1}	S	$\Delta\bar{\nu}_{1/2}$ (fwhm), cm^{-1}
[Re^{I}(4,4′-(CH$_3$)$_2$bpy)(CO)$_3$(4-Etpy)]$^+$	CH$_3$CN	18 600	18 500	1.4	2700
	PMMA	20 350	19 000	1.7	2180
[Re^{I}(bpy)(CO)$_3$(4-Etpy)]$^+$	CH$_3$CN	17 800	17 500	1.1	3000
	PMMA	20 000	18 870	1.6	2067
[Re^{I}(4,4′-(CO$_2$Et)$_2$bpy)(CO)$_3$(4-Etpy)]$^+$	CH$_3$CN	16 200	16 000	1.0	2500
	PMMA	18 400	17 600	1.2	2565

[a] $\hbar\omega$ was fixed at 1450 cm^{-1} in the spectral fits. The spectral fitting parameters are defined in the text with uncertainties of ±3% for E_0 and ±10% for S and $\Delta\bar{\nu}_{1/2}$. [b] As PF_6^- salts.

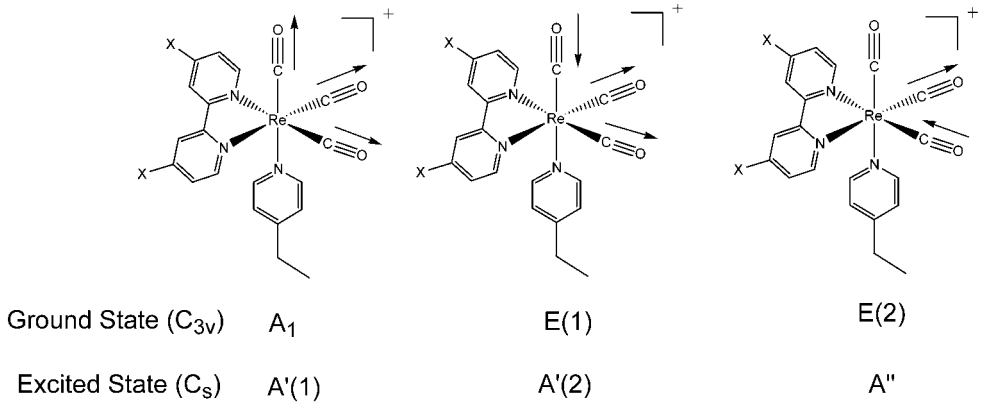

Figure 3. Local mode compositions of the normal modes for *fac*-[Re^{I}(4,4′-X$_2$bpy)(CO)$_3$(4-Etpy)]$^+$ in the ground (C_{3v}) and excited states (C_s).

is minimal. However, for MLCT excited states, the difference between frozen and fluid media can be large (Table 2 and results cited earlier).

ΔG°_{es}, can be calculated from E_0 by

$$\Delta G^\circ_{es} = E_0 + \lambda_{o,L} \tag{6}$$

with $\lambda_{o,L}$ related to the bandwidth at half-height ($\bar{\nu}_{1/2}$) for a single vibronic component in reciprocal centimeters by

$$(\bar{\nu}_{1/2})^2 = 16 k_B T \lambda_{o,L} \ln 2 \tag{7}$$

$\lambda_{o,L}$ includes contributions from the solvent and low-frequency modes treated classically. In fluid solution, $\lambda_{o,L}(fl) = \lambda_{oo} + \lambda_{io} + \lambda_{i,L}$, and in a rigid medium, $\lambda_{o,L}(fl) = \lambda_{o,L} + \lambda_{i,L}$.

On the basis of the similarity in MLCT absorption band energies for [Ru(bpy)$_3$]$^{2+}$ and related complexes in CH$_3$CN and PMMA, the frozen dielectric properties of the two are comparable.[15−17,22,51,52] Absorption is an instantaneous process on the time scale for nuclear motions, whether in solution or a rigid medium, and $E_{abs}(fr) - E_{abs}(fl) \sim 0$. $E_{abs}(fr)$ and $E_{abs}(fl)$ are the absorption band energies in rigid and fluid media, respectively.

Emission band energies are different in the two media for all but the most short-lived excited states. For long-lived excited states, the solvent is equilibrated and λ_{oo} is part of the solvent reorganizational energy rather than ΔG°. For an unstructured, Gaussian-shaped emission band the emission energies in rigid and fluid media are related by

$$E_{em}(fr) - E_{em}(fl) \sim 2\lambda_{oo}$$

λ_{oo} is related to the difference in E_0 between rigid and fluid media by

$$E_0(fr) - E_0(fl) = \lambda_{oo} \tag{8}$$

From the data in Table 2, and eq 8, $\lambda_{oo} = 1700$ (X = CH$_3$), 2100 (X = H), and 2200 cm^{-1} (X = CO$_2$Et). On the basis of the $\Delta\bar{\nu}_{1/2}$ values in Table 2, λ_{oo} is ∼50−80% of the total classical reorganization energy in solution.

MLCT Excited-State ν(CO) Spectra. The PMMA TRIR spectra in Figure 2 and Figure B in the Supporting Information have features in common with solution spectra.[1,3−6] In solution two bands appear in the ground state, arising from an A$_1$ mode and two unresolved E modes, as expected for pseudo-C_{3v} symmetry (Figure 3). The same ground-state pattern is observed in PMMA but there is evidence of an effective lowering of symmetry with separate components appearing at ∼1922 and ∼1930 cm^{-1} for the low-energy band.

In the Re^{II}(4,4′-X$_2$bpy$^{\bullet-}$) MLCT excited states, the local electronic symmetry is lowered to C_s because of the radical anion character of the acceptor ligand. Well-separated ν(CO) bands corresponding to A′(1), A′(2), and A″ modes appear in

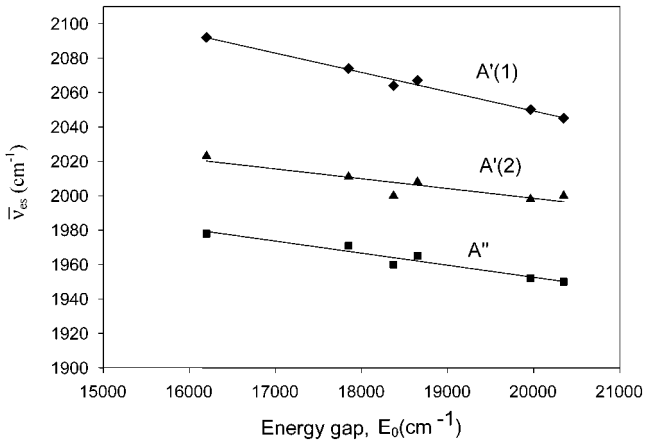

Figure 4. Plots of $\bar{\nu}_{es}$ vs E_0 for *fac*-[Re^{I}(4,4′-X$_2$bpy)(CO)$_3$(4-Etpy)]$^+$ in CH_3CN and PMMA for the A′(1) (◆), A′(2) (▲), and A″ (■) normal modes. The linear fits shown were to equations of slopes $\Delta\bar{\nu}_{es}/\Delta E_0 = -1.12 \times 10^{-2}$ for A′(1), -5.7×10^{-3} for A′(2), and -7.0×10^{-3} for A″ with the corresponding *y* intercepts 2.3×10^3, 2.1×10^3, and 2.1×10^3.

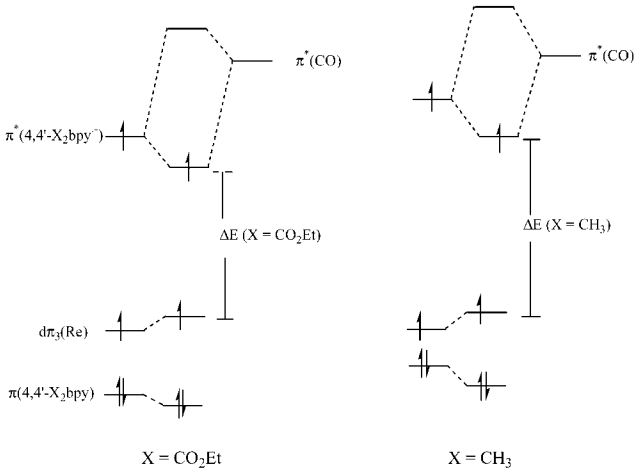

Figure 5. Schematic energy ordering diagram for the MLCT excited states illustrating π^*(4,4′-X$_2$bpy$^{\bullet-}$)−π^*(CO) and dπ_3(Re)−π(4,4′-X$_2$bpy) mixing for two cases: (1) X = CO_2Et and CH_3 and (2) X = CH_3 in CH_3CN and PMMA.

the TRIR spectra. In the excited state, the ordering is A′(1) > A′(2) > A″ with the ground-to-excited-state correlations $A_1 \rightarrow$ A′(1) and E → A″ + A′(2).[1,3−6] The largest ground-to-excited-state shift occurs for A′(2) with $\Delta\bar{\nu} = \bar{\nu}_{es} - \bar{\nu}_{gs} = +68$ cm^{-1}.

Ground-state ν(CO) band energies are essentially the same within experimental error in CH_3CN and PMMA (Table 2). There are significant differences between media in the excited states, with lower band energies systematically observed in PMMA. As shown by the data in Table 1, the decrease in PMMA compared to CH_3CN is 15−20 cm^{-1} for all three modes. These shifts are comparable to those observed by Turner and co-workers[13] between the fluid and frozen forms of 5:4 butyronitrile/propionitrile for *fac*-[Re^{I}(bpy)(CO)$_3$Cl] (−20, −18, and −23 cm^{-1}).

The change from CH_3CN to PMMA decreases $\bar{\nu}_{es}$ and increases the energy gap, E_0, derived by emission spectral fitting. There is a second way of changing the energy gap: by varying the substituent X in the series *fac*-[Re(4,4′-X$_2$bpy)(CO)$_3$(4-Etpy)]$^+$. As shown in a previous study, this is due to the electronic influence of X on the energy of the lowest π^* acceptor level.[13] It is apparent from the data in Table 1 that the variations in X also cause $\bar{\nu}_{es}$ to decrease as E_0 increases. It is important to note that $\bar{\nu}_{es}$ decreases as E_0 increases regardless of whether X or the medium is varied.

In Figure 4 are shown plots of $\bar{\nu}_{es}$ vs E_0 for all three ν(CO) bands and all three complexes *fac*-[Re(4,4′-X$_2$bpy)(CO)$_3$(4-Etpy)]$^+$ (X = CH_3, H, CO_2Et) in both media. These plots show that $\bar{\nu}_{es}$ decreases linearly with the energy gap to the same extent whether the medium or X is varied. This shows that the rigid medium effect is more generally an energy gap effect.

On the basis of the linear correlations in Figure 4, the sensitivities of the three normal modes to E_0 ($\Delta\bar{\nu}_{es}/\Delta E_0$) are -7.0×10^{-3} for A″, -5.7×10^{-3} for A′(2), and -11×10^{-3} for A′(1). For all three modes, $\bar{\nu}_{es}$ decreases as E_0 increases.

Orbital Basis for the Decrease in $\bar{\nu}_{es}$ with E_0. Electrochemical measurements on *fac*-[Re^{I}(4,4′-X$_2$bpy)(CO)$_3$(4-Etpy)]$^+$ (X = CH_3, H, and CO_2Et) in CH_3CN show that $E_{1/2}$(Re$^{II/I}$) reduction potentials [and the energy of the dπ^6(Re) levels] are relatively insensitive to changes in X.[16,17,22,51] The insensitivity to X also extends to dπ(Re)−π^*(CO) back-bonding as shown by the ν(CO) ground-state band energies in Table 1. On the basis of these observations, variations in E_0 are due largely to variations in the π^*(4,4′-X$_2$bpy) acceptor levels rather than to variations in dπ(Re). This causes the change in E_0 from CH_3CN to PMMA of ∼2000 cm^{-1}, which is comparable to the change in substituent from X = CH_3 to X = CO_2Et (Table 1).

On the basis of the arguments in a previous section, the increase in E_0 in PMMA is caused by the loss of stabilization of the excited state by orientational polarization. The orbital origin for this effect is presumably the same as the substituent effect in π^*(4,4′-X$_2$bpy) and can be explained qualitatively by use of the schematic energy level diagram in Figure 5. It illustrates substituent effects on orbital mixing in the MLCT excited states between the dπ_3(Re) hole level and π(4,4′-X$_2$bpy) and between π^*(4,4′-X$_2$bpy) and π^*(CO).

Figure 5 illustrates that the increase in E_0 for X = CH_3 compared to X = CO_2Et is largely due to the increase in π^*-(4,4′-X$_2$bpy). The orbital energy difference, ΔE, is related to E_0 and the pairing energy, P, by $E_0 = \Delta E - P$. The increase in π^*(4,4′-X$_2$bpy) decreases the π^*(4,4′-X$_2$bpy$^{\bullet-}$)−π^*(CO) energy gap, which enhances π^*(4,4′-X$_2$bpy$^{\bullet-}$)−π^*(CO) mixing and decreases $\bar{\nu}_{es}$.[16,17,22,51]

By inference, the rigid medium effect has the same origin. The loss of orientational polarization increases the energy of π^*(4,4′-X$_2$bpy) leading to enhanced π^*−π^* mixing. This suggests that the increase in E_0 and MLCT excited-state energies in rigid media is largely due to changes in polarization interaction at the ligand side of the excited-state dipole. This is reasonable since π^*(4,4′-X$_2$bpy$^{\bullet-}$) is on the periphery of the molecule.

Turner and co-workers initially attributed the rigid medium ν(CO) effect to mixing between MLCT and low-lying $\pi\pi^*$ states. On the basis of the arguments developed here, orbital mixing between π^*(4,4′-X$_2$bpy$^{\bullet-}$) and π^*(CO) provides an orbital basis for mixing between π^*(4,4′-X$_2$bpy$^{\bullet-}$)- and π^*(CO)-based MLCT states. It is this mixing that causes the rigid medium effect.

Mixing between the hole in dπ_3(Re) and π(4,4′-X$_2$bpy) is also illustrated in Figure 5 and shown as being of lesser magnitude given the small variations in $E_{1/2}$(Re$^{II/I}$) with X. It is greater for X = CH_3 since the energy gap between dπ_3(Re) and π(4,4′-X$_2$bpy) is less. It is this orbital interaction that provides the basis for MLCT [dπ(Re)−π^*(4,4′-X$_2$bpy)] mixing with $\pi\pi^*$ [π(4,4′-X$_2$bpy)−π^*(4,4′-X$_2$bpy)].

Conclusions

The decrease in ν(CO) with MLCT energy gap in the series *fac*-[Re^{I}(4,4′-X$_2$bpy)(CO)$_3$(4-Etpy)]$^{+}$* (X = CH_3, H, and CO_2-Et) are of similar magnitude whether variations are made in X or in medium between CH_3CN and PMMA. This points to a common orbital origin for the medium and substituent effects based on π*(4,4′-X$_2$bpy$^{\bullet-}$)−π*(CO) orbital mixing. With this interpretation, IR ν(CO) MLCT rigidochromism is a consequence of MLCT [dπ(Re)−π*(CO)] excited-state mixing with the emitting MLCT [dπ(Re)−π*(4,4′-X$_2$bpy)] excited states and not due to MLCT−$\pi\pi$* excited-state mixing.

Acknowledgment. We acknowledge the Department of Energy (Grant DE-FG02-96ER14607) and Los Alamos National Laboratory for funding this research. We also thank Cavan Fleming for incorporating complexes in PMMA matrices.

Supporting Information Available: Three figures showing the experimental setup for acquiring TRIR spectra, ground and time-resolved IR spectra of *fac*-[Re^{I}(4,4′-(CO$_2$Et)$_2$bpy)(CO)$_3$-(4-Etpy)]$^{+}$ in PMMA at 298 K in the ν(CO) region, and the emission spectrum of *fac*-[Re^{I}(bpy)(CO)$_3$(4-Etpy)]$^{+}$ in PMMA at 298 K. This information is available free of charge via the Internet at http://pubs.acs.org.

References and Notes

(1) Schoonover, J. R.; Strouse, G. E. *Chem. Rev.* **1998**, *98*, 1335−1355.
(2) Schoonover, J. R.; Bignozzi, C. A.; Meyer, T. J. *Coord. Chem. Rev.* **1997**, *165*, 239−266.
(3) Schoonover, J. R.; Strouse, G. F.; Omberg, K. M.; Dyer, R. B. *Comments Inorg. Chem.* **1996**, *18*, 165.
(4) Schoonover, J. R.; Strouse, G. F.; Dyer, R. B.; Bates, W. D.; Chen, P.; Meyer, T. J. *Inorg. Chem.* **1996**, *35*, 273−274.
(5) Turner, J. J.; George, M. W.; Clark, I. P.; Virrels, I. G. *Laser Chem.* **1999**, *19*, 245−251.
(6) Turner, J. J.; George, M. W.; Johnson, F. P. A.; Westwell, J. R. *Coord. Chem. Rev.* **1993**, *125*, 101.
(7) Omberg, K. M.; Dattelbaum, D. M.; Schoonover, J. R.; Meyer, T. J. Submitted for publication.
(8) Striplin, D. R.; Crosby, G. A. *Chem. Phys. Lett.* **1994**, *221*, 426−430.
(9) Kober, E. M.; Meyer, T. J. *Inorg. Chem.* **1984**, *23*, 3877−3886.
(10) Kober, E. M.; Meyer, T. J. *Inorg. Chem.* **1983**, *22*, 1614−1616.
(11) Braun, D.; Yersin, H. *Inorg. Chem.* **1995**, *34*, 1967.
(12) Kober, E. M.; Meyer, T. J. *Inorg. Chem.* **1982**, *21*, 3967.
(13) Clark, I. P.; George, M. W.; Johnson, F. P. A.; Turner, J. J. *Chem. Commun.* **1996**, 1587−1588.
(14) Wrighton, M. S.; Morse, D. L. *J. Organomet. Chem.* **1975**, *97*, 405−419.
(15) Zeng, J.; Hush, N. S.; Reimers, J. R. *J. Phys. Chem.* **1996**, *100*, 19292−19294.
(16) Vincze, L.; Friesen, D. A.; Mezyk, S. P.; Waltz, W. L. *Inorg. Chem.* **1992**, *31*, 4950−4958.
(17) Friesen, D. A.; Lee, S. H.; Nashiem, R. E.; Mezyk, S. P.; Waltz, W. L. *Inorg. Chem.* **1995**, *34*, 4026−4031.
(18) de Buyl, F.; Mesmaeker, A. K. *J. Photochem. Photobiol. A.* **1991**, *60*, 27−45.
(19) Chen, P.; Mecklenburg, S. L.; Duesing, R.; Meyer, T. J. *J. Phys. Chem.* **1993**, *97*, 13126−13131.
(20) Caspar, J. V.; Sullivan, B. P.; Kober, E. M.; Meyer, T. J. *Chem. Phys. Lett.* **1982**, *91*, 91−95.
(21) Caspar, J. V.; Meyer, T. J. *J. Am. Chem. Soc.* **1983**, *105*, 5583−5590.
(22) Timpson, C. J.; Bignozzi, C. A.; Sullivan, B. P.; Kober, E. M.; Meyer, T. J. *J. Phys. Chem.* **1996**, *100*, 2915−2925.
(23) Lee, A. J. *Comments Inorg. Chem.* **1995**, *17*, 319−346.
(24) Chen, P.; Meyer, T. J. *Inorg. Chem.* **1996**, *35*, 5520−5524.
(25) Chen, P.; Meyer, T. J. *Chem. Rev.* **1998**, *98*, 1439−1477.
(26) Worl, L. A.; Duesing, R.; Chen, P.; Della Ciana, L.; Meyer, T. J. *J. Chem. Soc., Dalton Trans.* **1991**, 849−858.
(27) Chen, P. Y.; Westmoreland, T. D.; Danielson, E.; Schanze, K. S.; Anthon, D.; Neveux, P. E.; Meyer, T. J. *Inorg. Chem.* **1987**, *26*, 1116.
(28) Chen, P.; Duesing, R.; Graff, D. K.; Meyer, T. J. *J. Phys. Chem.* **1991**, *95*, 5850−5858.
(29) Chen, P.; Palmer, R. A. *Appl. Spectrosc.* **1997**, *51*, 580−583.
(30) Claude, J. P.; Meyer, T. J. *J. Phys. Chem.* **1995**, *99*, 51−54.
(31) Kober, E. M.; Caspar, J. V.; Lumpkin, R. S.; Meyer, T. J. *J. Phys. Chem.* **1986**, *90*, 3722−3734.
(32) Huang, K.; Rhys, A. *Proc. R. Soc.* **1950**, *A204*, 406.
(33) Giordano, P. J.; Fredericks, S. M.; Wrighton, M. S.; Morse, D. L. *J. Am. Chem. Soc.* **1978**, *100*, 5051.
(34) Giordano, P. J.; Wrighton, M. S. *J. Am. Chem. Soc.* **1979**, *101*, 2888.
(35) Hager, G. D.; Crosby, G. A. *J. Am. Chem. Soc.* **1975**, *97*, 7031.
(36) Crosby, G. A.; Highland, R. G.; Truesdell, K. A. *Coord. Chem. Rev.* **1985**, *64*, 41.
(37) Burt, J. A.; Crosby, G. A. *Chem. Phys. Lett.* **1994**, *220*, 493.
(38) Fredericks, S. M.; Luong, J. C.; Wrighton, M. S. *J. Am. Chem. Soc.* **1979**, *101*, 7415.
(39) Jordan, K. J.; Wacholtz, W. F.; Crosby, G. A. *Inorg. Chem.* **1991**, *30*, 4588.
(40) Endicott, J. F.; Lessard, R. B.; Lynch, D.; Perkovic, M. W.; Ryu, C. K. *Coord. Chem. Rev.* **1990**, *97*, 65.
(41) Claude, J. P. Ph.D. Dissertation, The University of North Carolina at Chapel Hill, Chapel Hill, NC, 1995.
(42) Claude, J. P.; Williams, D. S.; Meyer, T. J. *J. Am. Chem. Soc.* **1996**, *118*, 9782.
(43) Schanze, K. S.; Walters, K. A. In *Molecular and Supramolecular Photochemistry*; Ramanurthy, V., Schanze, K. S., Eds.; Marcel Dekker: New York, 1998; Vol. 2.
(44) Stufkens, D. J.; Vlcek, A. *Coord. Chem. Rev.* **1998**, *177*, 127−179.
(45) Wrighton, M. S.; Morse, D. L. *J. Am. Chem. Soc.* **1974**, *96*, 998−1003.
(46) Lopez, R.; Leiva, A. M.; Zuloaga, F.; Loeb, B.; Norambuena, E.; Omberg, K. M.; Schoonover, J. R.; Striplin, D.; Devenney, M.; Meyer, T. J. *Inorg. Chem.* **1999**, *38*, 2924−2930.
(47) Fleming, G. R.; Cho, M. *Annu. Rev. Phys. Chem.* **1996**, *47*, 109.
(48) Marcus, R. A. *J. Phys. Chem.* **1989**, *93*, 3078.
(49) Marcus, R. A.; Sutin, N. *Biochim. Biophys. Acta* **1985**, *811*, 265−322.
(50) Papazyan, A.; Maroncelli, M. *J. Chem. Phys.* **1995**, *102*, 2888−2919.
(51) Caspar, J. V.; Meyer, T. J. *J. Am. Chem. Soc.* **1983**, *105*, 5583.
(52) Hush, N. S.; Reimers, J. R. *Coord. Chem. Rev.* **1998**, *177*, 37−60.